Interaction between Resonant Magnetic Perturbations and Transport Barriers

A. Monnier[1], G. Fuhr[1], P. Beyer[1], S. Benkadda[1]

[1] *Aix-Marseille Univ., CNRS, PIIM UMR 7345, 13397, Marseille, France*

The control of Edge Localized Modes (ELMs) [1] in tokamaks is a key issue for fusion plasma regimes. These regimes are characterised by transport barriers, more precisely a thin layer where the turbulent transport of heat and density is significantly reduced leading to a strong increase of pressure gradient. Localized at the edge, this barrier is not stable and exhibits quasi-periodic relaxations with important energy fluxes, eventually dangerous for the tokamak wall. These relaxations are a characteristic of ELMs. Several techniques have been suggested to stabilize or remove these relaxations [2] in the next tokamak ITER. One promising method is based on external Resonant Magnetic Perturbations (RMPs) at the plasma edge. These magnetic perturbations reveal a qualitative control in the DIII-D [3], JET [4] and TEXTOR [5] experiments.

The control of transport barrier relaxations by RMPs is generally due to a reduction of pressure gradient by a radial energy flux [6]. This property is attributed to the appearence of field line stochasticity for large RMP amplitudes. However, it is not clear to which extend the externally induced perturbation actually penetrates into the plasma. Magnetohydrodynamical (MHD) modeling has shown an effective screening of RMPs by a rotating plasma [7]. This screening has also been observed in numerical simulations with an effective velocity at the plasma edge [8].

In previous works, control of barrier relaxations have been studied by three-dimensional edge turbulent simulations in presence of externally induced RMPs [9]. Recently, an extension of the previous electrostatic model was used taking into account self-consistent electromagnetic fluctuations [10]. The aim was to study the penetration of RMP into the plasma. In the present work, the impact of RMPs on a turbulent plasma in presence of an $\mathbf{E}\times\mathbf{B}$ flow will be studied. in particular, a shear flow sufficient to generate an edge transport barrier is taken into account.

The model equations used for the plasma pressure p, the electrostatic potential ϕ and the electromagnetic flux ψ are :

$$(\partial_t + \vec{\mathbf{u}}_E\cdot\nabla)\,W = -\frac{1}{\alpha}\nabla_\parallel J - \mathbf{G}p + \nu\nabla_\perp^2 W + \mu\,(W_{00} - W_{imp})\,, \quad (1)$$

$$(\partial_t + \vec{\mathbf{u}}_E\cdot\nabla)\,p = \delta_c\mathbf{G}\phi + \chi_\parallel\nabla_\parallel^2 p + \chi_\perp\nabla_\perp^2 p + S(x), \quad (2)$$

$$\partial_t\psi = -\nabla_\parallel\phi + \frac{1}{\alpha}\,(J - J_{RMP})\,. \quad (3)$$

Equation (1) corresponds to the vorticity equation, $W = \nabla_\perp^2\phi$ is the vorticity of the $\mathbf{E}\times\mathbf{B}$ flow $\vec{\mathbf{u}}_E$, $J = \nabla_\perp^2\psi$ is the parallel current fluctuation, α is proportional to the plasma β, i.e. the ratio of kinetic to magnetic pressure. $\mathbf{G}$ is the magnetic curvature operator, ν is the viscosity coefficient, μ is the friction coefficient with the imposed vorticity $W_{imp} = \nabla_\perp^2 \phi_{imp} = \partial_x^2 \phi_{imp}$. W_{00} corresponds to the axisymmetric component of W. Eq. (2) describes the energy conservation, $\chi_\parallel$ and $\chi_\perp$ are respectively the collisional heat diffusivities parallel and perpendicular to the magnetic field lines, δ_c is a curvature parameter, and $S(x)$ is an energy source modeling the constant heat flux from the plasma core. Eq. (3) corresponds to the Ohm's Law, J_{RMP} is the external current source generating RMPs. Simultations are performed with the EMEDGE3D code [11]. Following the standard convention x, y, z represent respectively the normalized local radial, poloidal and toroidal coordinates. Introducing the safety factor q, the main computational domain corresponds to the volume delimited by the toroidal surfaces $q_{min} = 2.5$ and $q_{max} = 3.5$ (Fig. 1a, vertical black dash lines). The energy source $S(x)$ is located in the region $q < q_{min}$.

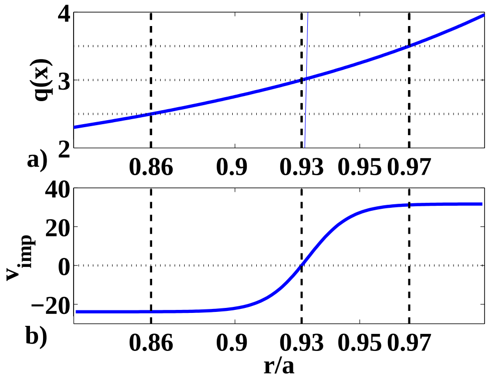

Figure 1: Radial profiles of safety factor q (a), and imposed $\mathbf{E}\times\mathbf{B}$ flow v_{imp} (b).

In recent work [10], the penetration of RMP has been studied in two cases : first in a quiescent plasma, with or without imposed poloidal rotation. Second, a turbulent plasma has been considered with important energy source, driving the pressure gradient above the resistive ballooning instability threshold. Results show an effective screening due to the poloidal rotation profile. When the poloidal rotation vanishes at the resonant RMP position, the screening decreases strongly. The RMP penetration in turbulent plasma exhibits an effective amplification generated by the turbulence. In presence of imposed poloidal rotation, a partial penetration of RMP is observed.

We study the effect of RMPs on turbulent plasma in presence of imposed $\mathbf{E}\times\mathbf{B}$ rotation. This imposed poloidal rotation profile is sufficient to generate a transport barrier (Fig. 1b, labelled $v_{imp} = \partial_x \phi_{imp}$).

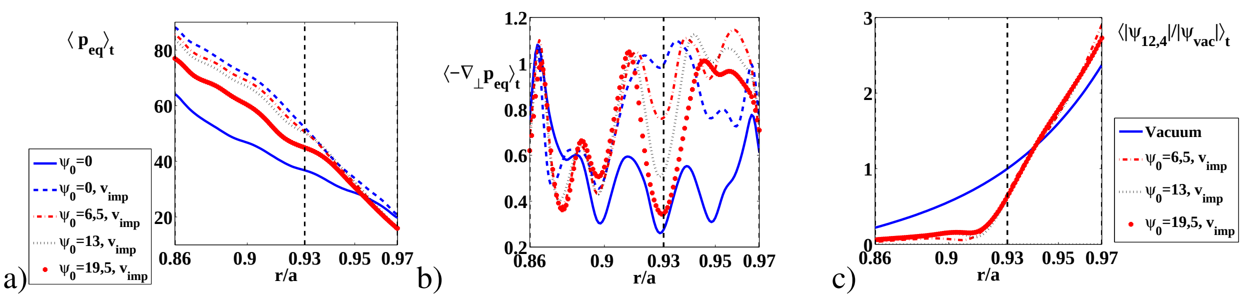

Figure 2: Radial profiles of p_{eq} (a), $\nabla_\perp p_{eq}$ (b) , and screening factor (c) for different values of ψ_0 and reference cases.

The external RMP source is chosen to be resonant at the magnetic surface $q_0 = 3$ (corresponding to

$r/a \approx 0.93$) with the poloidal and toroidal mode number $m_0 = 12$ and $n_0 = 4$, respectively, for three different RMP amplitudes $\psi_0 = 6.5; 13; 19.5$. The imposed poloidal rotation v_{imp} vanishes at the position $q = 3$ to allow the RMP penetration [10] and defines the barrier position. Two reference cases are defined by the turbulent plasma without RMP, in presence or not of imposed poloidal rotation (labelled $\psi_0 = 0$ and $\psi_0 = 0, v_{imp}$). A vacuum case has been defined (without plasma reponse in the Ohm's Law), to quantify the screening via the factor $S_{mn} = |\psi_{mn}|/|\psi_{mn}^{vac}(q=m/n)|$ where ψ_{mn} corresponds to the Fourier component of ψ for the poloidal and toroidal mode number (m, n), respectively .

Numerical simulations lead to statistically stationary states. The time average of the equilibrium pressure shows an enhanced pressure gradient in presence of the $\mathbf{E} \times \mathbf{B}$ rotation (Fig. 2a and b, blue dash line) compared to the reference turbulent case without imposed rotation (full blue line). In presence of RMP (red and black curve), the pressure decreases in the inner region $q < q_0$ with the RMP amplitude ψ_0. This can be attributed to a local reduction of the pressure gradient (Fig. 2b) exhibits in presence of RMP at the the position $r/a \approx 0.93$ (q_0). This local flattening, increasing with the RMP source amplitude, is due to the partial penetration of RMP in the plasma (Fig. 2c). The local reduction of the pressure gradient in presence of RMP is essential for the control of transport barrier relaxations like ELMs.

The local reduction of $\nabla_\perp p_{eq}$ can be explained by the flux balance obtained from the energy equation (Eq. 2). If we consider the spatial average in poloidal and toroidal directions of the energy equation, we obtain :

$$\partial_t p_{eq} = -\partial_x \left[\left\langle p \partial_y \phi \right\rangle_{y,z} - \chi_\parallel \left\langle \partial_y \psi \nabla_\parallel p \right\rangle_{y,z} - \chi_\perp \partial_x p_{eq} \right] + S(x),$$

where $p_{eq} = \langle p \rangle_{y,z}$. For a steady state, we integrate in radial direction x :

$$Q_{conv}^{turb} + Q_{\Delta B} + Q_{coll} = Q_{tot},$$

with $Q_{conv}^{turb} = \left\langle p \partial_y \phi \right\rangle_{y,z}$, the turbulent convective flux, $Q_{\Delta B} = -\chi_\parallel \left\langle \partial_y \psi \nabla_\parallel p \right\rangle_{y,z}$, the parallel heat flux on magnetic field lines, $Q_{coll} = -\chi_\perp \partial_x p_{eq}$, the collisional flux and the total heat flux $Q_{tot} = \int S(x)\, dx$. In presence of RMP (Fig. 3a), the time average of the convective flux and the parallel heat flux (Fig. 3b) are roughly unchanged near the resonant surface q_0 when increasing the RMP amplitude. If we consider the stationary part of the convectif flux, we can write :

$$\langle Q_{conv} \rangle_t = Q_{conv}^{stat} + \left\langle Q_{conv}^{turb} \right\rangle_t ,$$

The stationary component of the convective flux $Q_{conv}^{stat} = \left\langle \langle p \rangle_t \, \partial_y \langle \phi \rangle_t \right\rangle_{y,z}$ (Fig. 3c) is identified to be at the origin of the local flattening of the pressure gradient, proportionnal to the collisional flux. The stationary convective flux is important near the resonant surface q_0 ($r/a = 0.93$), and increases

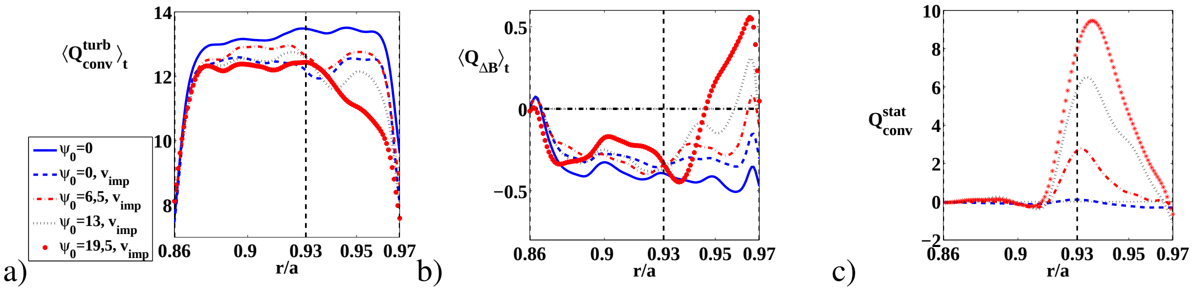

Figure 3: Radial profiles of time average of Q_{conv} (a), $Q_{\Delta B}$ (b) and Q_{conv}^{stat} (c) for different values of ψ_0 and reference cases.

with the RMP amplitude. As the parallel heat flux does not change significantly with the RMP at the barrier position and the total heat flux is constant, the local flattening of pressure gradient (collisional heat flux) is essentially due to Q_{conv}^{stat}.

To conclude, when RMP is applied on turbulent plasma with transport barrier, the 3D simultations show a partial penetration of the imposed magnetic perturbation [10]. In presence of RMPs, a local flattening of the pressure gradient is observed, explained by the generation of stationary convective flux associated with the magnetic perturbation. This flux induces a local erosion of the pressure gradient on the RMP resonant surface. These results show that transport due to stationary convection cells associated with the magnetic perturbation can contribute significantly to the local reduction of the pressure gradient at the transport barrier. The latter is known to be at the origin of the control of barrier relaxations by RMPs. The work on the demonstration of effective control in 3D turbulence simulations with self-consistent RMP penetration is in progress.

This work has been supported by the French National Research Agency, project ANR-2010-BLAN-940-01. This work was granted access to the HPC resources of Aix-Marseille Université financed by the project Equip@Meso (ANR-10-EQPX-29-01) of the program "Investissements d'Avenir" supervised by the Agence Nationale pour la Recherche.

References

[1] Connor J.W. 1998 Plasma Phys. Control. Fusion **40** 531
[2] Hawryluk R. *et al.* 2009 Nucl. Fusion **49** 065012
[3] T.E. Evans et al., Phys. Rev. Lett. **92**, 235003 (2004).
[4] Liang Y. *et al.* 2007 Phys. Rev. Lett. **98** 265004
[5] Finken K.H. *et al.* 2007 Nucl. Fusion **47** 522
[6] Bécoulet M. *et al.* 2005 Nucl. Fusion **45** 1284
[7] Nardon E. *et al.* 2007 Phys. Plasmas **14** 092501
[8] Bécoulet M. *et al.* 2012 Nucl. Fusion **52** 054003
[9] Beyer P. *et al.* 2011 Plasma Phys. Control. Fusion **53** 054003
[10] Monnier A. *et al.* 2014 Nucl. Fusion **54** 064018
[11] Fuhr G. *et al.* 2008 Phys. Rev. Lett. **101** 195001